THE JOURNAL OF PHYSICAL CHEMISTRY Letters

Letter

pubs.acs.org/JPCL

Platinum Monolayer Electrocatalysts for Anodic Oxidation of Alcohols

Meng Li, Ping Liu, and Radoslav R. Adzic*

Department of Chemistry, Brookhaven National Laboratory, Upton, New York 11973, United States

Supporting Information

ABSTRACT: The slow, incomplete oxidation of methanol and ethanol on platinum-based anodes as well as the high price and limited reserves of Pt has hampered the practical application of direct alcohol fuel cells. We describe the electrocatalysts consisting of one Pt monolayer (one atom thick layer) placed on extended or nanoparticle surfaces having the activity and selectivity for the oxidation of alcohol molecules that can be controlled with platinum-support interaction. The suitably expanded Pt monolayer (i.e., Pt/Au(111)) exhibits a factor of 7 activity increase in catalyzing methanol electrooxidation relative to Pt(111). Sizable enhancement is also observed for ethanol electrooxidation. Furthermore, a correlation between substrate-induced lateral strain in a Pt monolayer and its activity/selectivity is established and rationalized by experimental and theoretical studies. The knowledge we gained with single-crystal model catalysts was successfully applied in designing real nanocatalysts. These findings for alcohols are likely to be applicable for the oxidation of other classes of organic molecules.

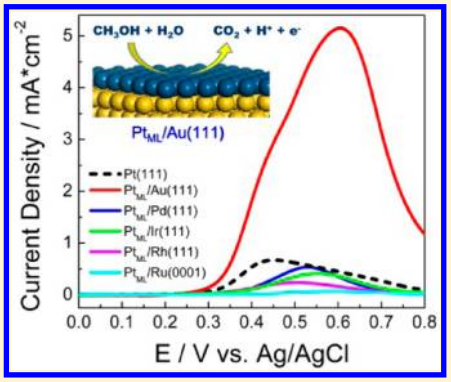

SECTION: Surfaces, Interfaces, Porous Materials, and Catalysis

Many problems encountered in hydrogen-fuel-cell technology, particularly those of hydrogen storage and distribution, can be circumvented by replacing hydrogen with liquid fuels, such as methanol and ethanol.[1,2] The slow and incomplete electrocatalytic oxidation reaction of these alcohol molecules occurring at the fuel-cell anode is the main impediment to practical application of the direct alcohol fuel cell (DAFC).[3,4] Platinum and Pt-based materials are currently the best electrocatalysts for these reactions. The price and the limited reserves of Pt are the prime obstacles to adequately developing this major field.

Extensive research efforts have been devoted to enhance the Pt-based catalysts, yet despite significant advances in recent years the activity of existing catalysts is still inadequate and the Pt content is high. Structural effects in these reactions were well-established, and the different activities of the Pt surfaces with different crystallographic orientations afforded the possibility of optimizing the catalysts' surface.[5−12] Other strategies include alloying Pt with a second element and incorporating active cocatalysts such as adatoms and metal oxides.[13−15] We developed Pt monolayer (Pt_{ML}) electrocatalysts comprising one atom thick layer of Pt placed on extended or nanoparticle surfaces and inaugurated these catalysts for the oxygen reduction reaction (ORR).[16−18] The electrochemical behavior of electrodeposited Pd overlayers on different single-crystal substrates was studied for reactions such as hydrogen desorption and formic-acid oxidation.[19,20] Most recently considerable research was undertaken in computing the effects of structural changes in the surface upon its reactivity.[21,22]

In this letter we describe the successful application of the Pt_{ML} concept in the electrooxidation of methanol and ethanol. It facilitates decreasing the Pt content to a single monolayer and in parallel the tuning of the catalytic properties of such monolayers for alcohol oxidation. Accelerating these reactions on a Pt_{ML} is provoked by its interaction with an adequate substrate. A correlation between substrate-induced lateral strain in Pt_{ML} and its activity has been established, and the results are in full agreement with theoretical prediction. We also demonstrate the applicability of the knowledge attained from single-crystal-based model catalysts study for the design of real nanocatalysts.

We synthesized these electrocatalysts by depositing a Pt monolayer on different substrates via the galvanic displacement of an underpotentially deposited (UPD) Cu monolayer (Figure S1 of the Supporting Information) employing five single-crystal surfaces (Au(111), Pd(111), Ir(111), Rh(111), and Ru(0001)) as substrates.[24] Structures and morphologies of the resulted monolayers of Pt have been characterized by scanning tunneling microscopy (STM) studies (vide infra).[24,25] By selecting the suitable substrate, we can tailor the electrocatalytic properties of Pt_{ML} consequent upon the combined geometric effect (substrate-induced strain) and ligand effect (the electronic interaction between Pt_{ML} and the substrate). Figure 1 displays linear sweep voltammetry curves for Pt_{ML} electrocatalysts together with Pt(111) during the methanol- (MOR)

Received: October 9, 2012
Accepted: November 12, 2012
Published: November 12, 2012

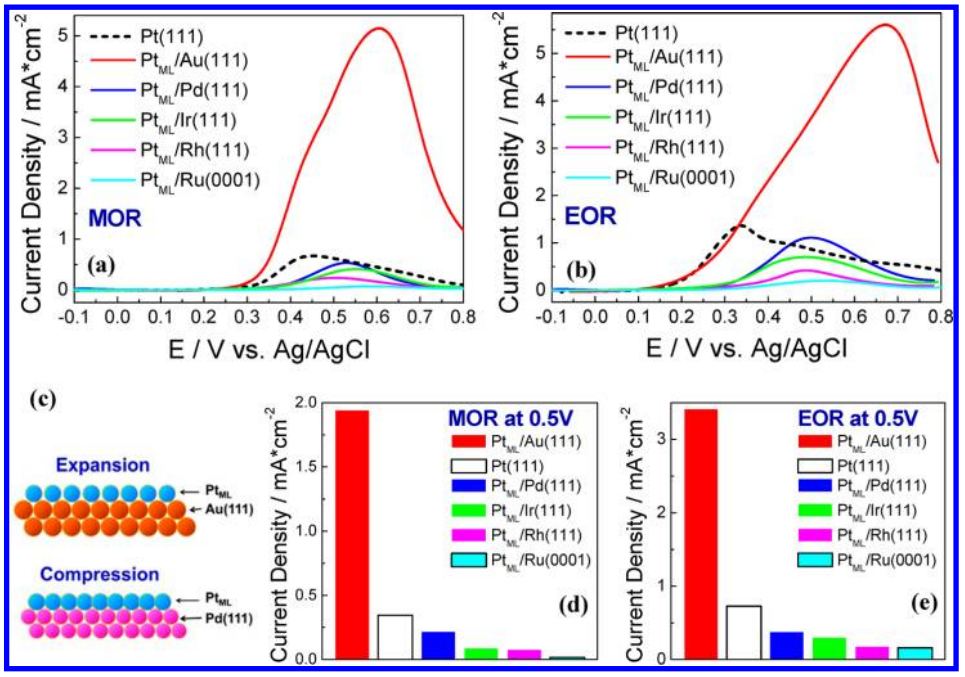

Figure 1. Schematic illustration and electrochemical studies of single-crystal Pt_{ML} model catalysts. Positive voltammetric scans for Pt(111) and Pt_{ML} supported on five different substrates in 0.1 M $HClO_4$ containing 0.5 M methanol (a) or 0.5 M ethanol (b) with scan rate 10 mV/s. (c) Models of pseudomorphic monolayers of Pt on two different substrates of Au(111) and Pd(111). Current densities measured at 0.5 V in quasi-steady state conditions at a sweep rate of 1 mV/s during MOR (d) and EOR (e). Currents are normalized to the measured Pt surface area, which is determined by the charge of stripping one Cu UPD monolayer on Pt(111) or Pt_{ML} (assuming 480 $\mu C/cm^2_{Pt}$).[23].

and ethanol-oxidation reaction (EOR). Taking as examples a $Pt_{ML}/Au(111)$ surface, where Au exerts on Pt a tensile strain, and a $Pt_{ML}/Pd(111)$ surface where Pt is under compressive strain (schematic illustration in Figure 1c), we demonstrated a significant enhancement in the catalytic activity associated with the tensile strain and decreased activity associated with the compressive strain. During the MOR (Figure 1a), the $Pt_{ML}/Au(111)$-, $Pt_{ML}/Pd(111)$-, and Pt(111)-surfaces, respectively, show reaction onset potentials (measured at 0.05 $mA*cm^{-2}$) of 0.25, 0.37, and 0.29 V and a peak current density in anodic potential scans of 5.12 (at 0.61 V), 0.45 (at 0.53 V), and 0.67 $mA*cm^{-2}$ (at 0.45 V). Hence, $Pt_{ML}/Au(111)$ exhibits a negatively shifted potential at the onset of the reaction and over seven-fold enhancement in peak current density with respect to Pt(111) (the most active low-index plane of Pt[5−7]). Similarly, during the EOR (Figure 1b), the stretched Pt_{ML} supported on Au(111) demonstrates slightly negatively shifted reaction-onset potential and over four-fold increase in peak current density. Figure S2 of the Supporting Information summarizes the complete results from voltammetry study and slow-sweep-rate polarizations from all catalytic surfaces. We plot the current densities measured at 0.5 V in quasi-steady-state conditions at a sweep rate of 1 mV/s during MOR (Figure 1d) and EOR (Figure 1e) to verify the substrate-induced change in the activity of Pt_{ML}. A trend that increased lattice compression lowers reactivity is observed. Significant structure sensitivity of the oxidation of small organic molecules, including methanol and ethanol, has been well-established in studies involving well-defined low-index[5−7] and high-index Pt single-crystal surfaces.[8−12] The question arises whether 2-dimensional (2D) Pt islands can act as steps in Pt-stepped surfaces and cause enhanced rates. This can be ruled out as a possibility for the following reasons. First, the step density on well-ordered Au(111) is not high, and even if Pt forms islands it will not make step density comparable to those of high-index planes. A recent study by Brankovic's group shows that in the submonolayer range of Pt deposits smaller 2D islands have smaller tensile strain and smaller activity for hydrogen oxidation reaction.[26] Thus, the effect of steps of Pt deposit would have the opposite effect. In our experiment, the size of Pt islands should be considerable because one Cu atom is displaced by one Pt^{2+}. Second, if steps were contributing to the activity, then that should be observed with Pt monolayer on other four metal surfaces (i.e., Pd(111), Ir(111), Rh(111), Ru(0001)), not only for Pt/Au(111). The high activity of Pt−Au system for reactions like CO oxidation and formic acid oxidation was interpreted in several different ways.[26−28]

Methanol and ethanol electrooxidation are complex reactions occurring in a pattern of parallel reaction pathways. The overall MOR and EOR are formulated as follows

$$CH_3OH \rightarrow (\text{adsorbed intermediates}) \rightarrow CO_2, HCHO, \text{and } HCOOH$$

$$CH_3CH_2OH \rightarrow (\text{adsorbed intermediates}) \rightarrow CH_3CHO, CH_3COOH, CO_2, \text{and } CH_x$$

A complete oxidation to CO_2 of organic molecules is necessary in energy-conversion applications; that is, both the MOR and the EOR require a catalyst that can (i) adsorb these molecules, (ii) dissociate the C−H bond and split the C−C bond in ethanol, and (iii) dissociate water to facilitate the reaction of the resulting alcohol adsorbates with oxygen-containing species to form CO_2 (or HCOOH, CH_3CHO, CH_3COOH). We undertook an in situ infrared reflection absorption spectroscopy (IRRAS) study to identify the reaction intermediates and products during MOR and EOR on $Pt_{ML}/Au(111)$ to gain insight into the substrate-induced change in

dx.doi.org/10.1021/jz3016155 | J. Phys. Chem. Lett. 2012, 3, 3480−3485

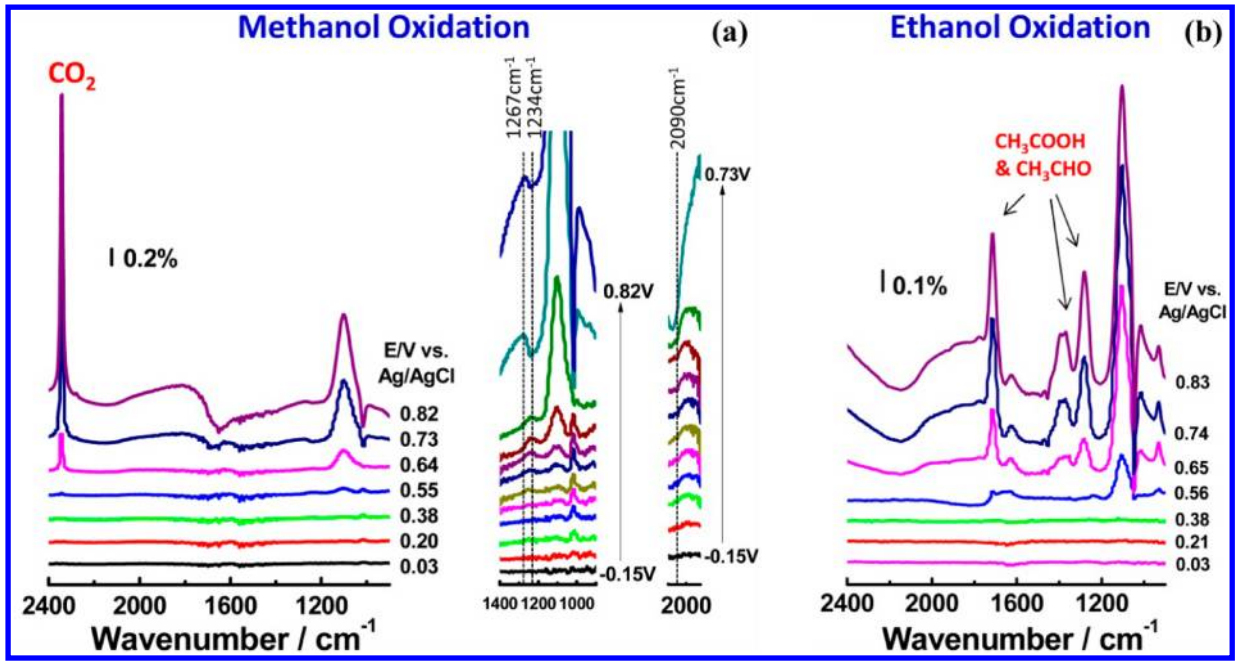

Figure 2. In situ IRRAS spectra for identifying the intermediates and products of methanol and ethanol electrooxidation on $Pt_{ML}/Au(111)$. In situ IRRAS spectra recorded during MOR (a) and EOR (b) on the $Pt_{ML}/Au(111)$ electrode in 0.1 M $HClO_4$ containing 0.5 M methanol or 0.5 M ethanol. 128 interferograms (resolution 8 cm^{-1}) were coadded to each spectrum.

the selectivity of Pt_{ML} and into the mechanism of the greatly enhanced reaction kinetics.

Figure 2a displays the in situ IRRAS spectra recorded on $Pt_{ML}/Au(111)$ during MOR. The detailed band assignments are given in Table S1 of the Supporting Information. The strong band at around 2343 cm^{-1} is ascribed to CO_2, indicating that the main MOR product is CO_2. A close look at 1800−2100 and 900−1400 cm^{-1} regions is also included in Figure 2a. A weak band at ∼2090 cm^{-1} can be assigned to linearly bonded CO (CO_L), and the low intensity of CO_L indicates a minimum amount of poison species. We assigned the band at 1267 cm^{-1} to some H-containing intermediate, possibly COH_{ads}.[29,30] The band at 1234 cm^{-1} is due to O−C−O stretching in methyl formate, and it partially overlaps with the COH_{ads} band. The band at 1010 cm^{-1} reflects C−O stretching in methanol adsorbates and also in solution methanol. Methanol oxidation on a Pt electrode can be described as a multistep reaction generating several intermediates and products:

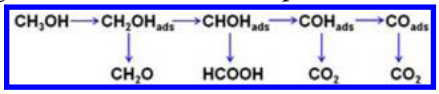

Previous FTIR studies demonstrated the existence of adsorbed CO (CO_{ads}) and the formation of formic acid (indicated as the carbonyl group at ∼1710 cm^{-1}) during the MOR on single-crystal and polycrystalline platinum electrodes.[6,29,30] Meanwhile, the absence of carbonyl group bands, as well as the existence of a COH_{ads} band, indicates that methanol oxidation on $Pt_{ML}/Au(111)$ tends to be further dehydrogenated to COH_{ads} instead of being oxidized to formaldehyde and/or formic acid. In addition, the low intensity of CO_{ads} band implies that COH_{ads} can be oxidized directly to CO_2 rather than forming CO_{ads}. Our voltammetry study (Figure S3 of the Supporting Information) in agreement with previous reports[16,31] revealed a higher oxygen adsorption/desorption current (i.e., a higher OH coverage) on the expanded $Pt_{ML}/Au(111)$ compared with the compressed $Pt_{ML}/Pd(111)$. The increased −OH formation on $Pt_{ML}/Au(111)$ could promote the oxidation of COH_{ads}. Therefore, spectroscopic study shows that the enhanced MOR activity on this catalyst is due to the formation of COH_{ads} instead of poisoning CO_{ads} and the promoted oxidation of COH_{ads} directly to CO_2.

Figure 2b presents the IRRAS spectra collected during the EOR. The main feature is the absence of both the CO_{ads} and CO_2 bands, denoting that ethanol dissociative adsorption on $Pt_{ML}/Au(111)$ does not occur and that the EOR follows partial oxidation pathway without cleavage of the C−C bond.[32] The complete oxidation of ethanol requires full dehydrogenation and C−C bond splitting, which might not be favored on stretched Pt_{ML}. We can assign the band located around 1705 cm^{-1} to the stretch vibration of the C═O bond, found in both acetaldehyde and acetic acid. The well-defined band at 1280 cm^{-1} is the characteristic absorption of C−O stretching in acetic acid. The bands at 1350 cm^{-1} and around 1396−1410 cm^{-1}, respectively, reflect the CH_3 in-plane bending mode and O−C−O stretching of adsorbed acetate. The band observed at 933 cm^{-1} is assigned to the C−C−O asymmetric stretching of acetaldehyde. Hence, we ascribe the high EOR activity on $Pt_{ML}/Au(111)$ to the fast kinetics of partial oxidation pathway generating acetic acid and acetaldehyde. The spectroscopic studies of Pt_{ML} electrocatalysts on other supports are in progress in our laboratory.

The ligand effect is probably contributing to the observed activity. For metal overlayers a combination of ligand and strain effect is usually found. They are difficult to separate and the d-band centers are found to describe changes in adsorption energies well.[21,22] Our study reveals a correlation between the lateral strain and reactivity.

We carried out DFT calculations to gain better understanding of the methanol electrooxidation on the surfaces of $Pt_{ML}/Cu(111)$, Ru(001), Rh(111), Re(001), Pd(111), Os(001), Ir(111), Ag(111), and Au(111) (Figure 3). Previous DFT studies by Mavrikakis and coworkers showed two

dx.doi.org/10.1021/jz3016155 | J. Phys. Chem. Lett. 2012, 3, 3480−3485

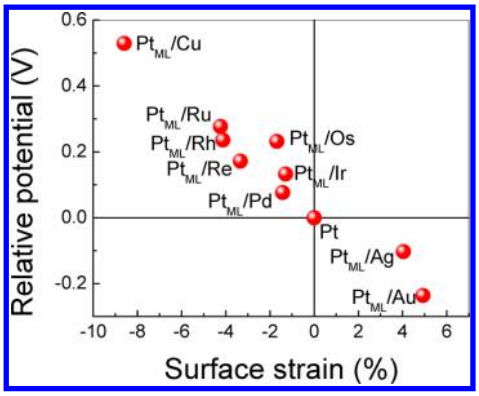

Figure 3. DFT investigations of methanol oxidation on Pt_{ML} supported on different substrates. The DFT-calculated variation of the lowest potential to proceed methanol electrooxidation on the Pt_{ML} supported on Cu(111), Ru(001), Rh(111), Re(001), Pd(111), Os(001), Ir(111), Ag(111), Au(111) surfaces with the surface strain. The surface stain was calculated by $[d(Pt_{ML/surf}) - d(Pt)]/d(Pt)$, where d is Pt−Pt bond length. The potential and surface strain are expressed with respect to the case of Pt(111).

mechanisms for methanol oxidation to CO_2 on pure metal surfaces: an indirect mechanism via a CO intermediate and a direct mechanism wherein methanol is oxidized to CO_2 without forming a CO intermediate.[33,34] They identified the free energies of OH and CO as being the key descriptors, able to determine the onset potential for methanol electrooxidation. On the basis of their work, we estimated the onset potential for methanol electrooxidation on the Pt_{ML}/metal surfaces by calculating the binding energies and free energies of CO and OH. Our results show that among the systems studied, the direct mechanism is preferred energetically and the potential-determining step is the dehydrogenation of methanol to hydroxymethyl. The only exception is Pt_{ML}/Re(001), wherein the indirect mechanism is favored slightly; this finding agrees well with the experimental ones, showing low intensity of CO_{ads} band for methanol oxidation on the surfaces. In addition, the onset potential for methanol electrooxidation correlates well with the surface strain that affects the binding activities of Pt_{ML}. Norskov et al. reported that the characteristics of the surface metal d-bands, particularly the weighted center of the d-band (ε_d), play a decisive role in determining surface reactivity.[21,22] A higher-lying ε_d characterizes a more reactive surface that tends to bind adsorbates more strongly and enhances the kinetics of dissociation reaction producing these adsorbates. A surface with a lower-lying ε_d tends to bind adsorbates more weakly and facilitates the formation of bonds among them. In agreement with the previous calculations,[18,21] we also observed that the positive- or tensile-surface strain in the metal overlayer tends to upshift εd in energy and therefore increases the CO- and OH-binding energy. Pt_{ML}/Au(111) and Pt_{ML}/Ag(111) are the only two surfaces in our study that display tensile strain compared with Pt(111) and enhance the reactivity of Pt. The stretched Pt−Pt bonds induced by the support metals strengthen the Pt−CO and Pt−OH bonds. For instance, when going from Pt(111) to Pt_{ML}/Au(111), the binding of CO and OH is increased, respectively, by 0.4 and 0.13 eV, and, therefore, the onset potential for methanol oxidation is lowered by 0.24 eV according to the formalism in the previous studies.[33] On the contrary, using, for example, the Cu and Pd supports that introduce compression to Pt_{ML} results in a lower activity than Pt(111). The DFT-predicted trend in reactivity agrees well with the experimental observations, showing in decreasing sequence, Pt_{ML}/Au(111) > Pt(111) > Pt_{ML}/Pd(111) > Pt_{ML}/Ir(111) > Pt_{ML}/Rh(111) > Pt_{ML}/Ru(0001); Pt_{ML}/Au(111) displays the highest activity, where Pt_{ML} is stretched by over 4% and exhibits enhanced reactivity in the dehydrogenative adsorption of alcohol molecules (Pt−CO) and the dissociation of water (Pt−OH formation). That is, the strain effect due to the Au support results in a Pt with moderate activity being able to bind the adsorbates strongly enough to activate methanol, yet weakly enough to prevent CO poisoning and allow the formation of CO_2.

Finally, to demonstrate the generality of the behavior found with single-crystal surfaces, we designed several Pt_{ML} nanocatalysts comprising Pt_{ML} supported on mono- or bimetallic nanoparticle cores. Figure 4 presents anodic polarization curves for Pt_{ML} nanocatalysts and Pt/C during MOR and EOR. The activity for both reactions increases in the order of Pt_{ML}/Pd/C < Pt/C < Pt_{ML}/Au/C. Hence, a qualitatively similar trend is observed as with single-crystal surfaces; namely, dilated Pt_{ML} enhances activity while activity in compressed Pt_{ML} is decreased. Pt_{ML} supported on Pd−Au bimetallic alloy nanoparticles demonstrates an activity in between Pt_{ML}/Pd/C and Pt_{ML}/Au/C, which also suggests that a tunable activity can be obtained from Pt_{ML} by manipulating its lateral strain. Nanoparticles are generally enclosed by a mixture of (111)

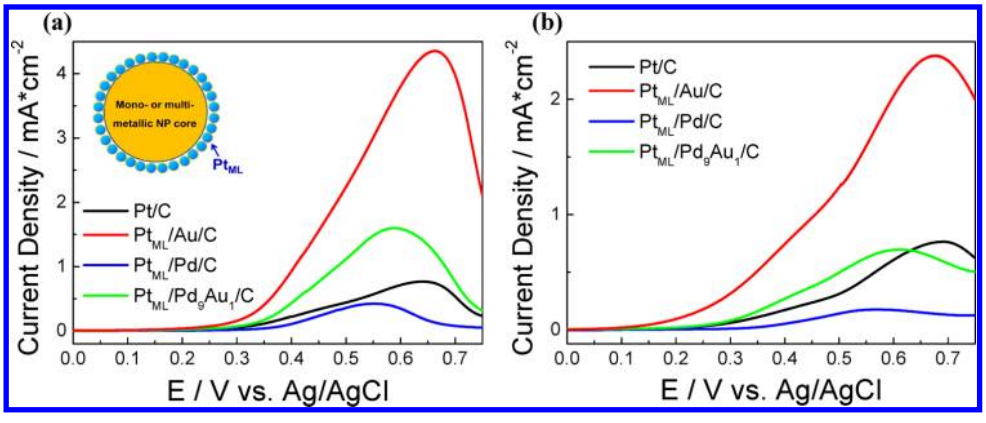

Figure 4. Electrochemical studies of several Pt_{ML} nanocatalysts. Positive voltammetric scans for Pt/C and Pt_{ML} supported on different nanoparticle substrates in 0.1 M $HClO_4$ containing 0.5 M methanol (a) or 0.5 M ethanol (b) with scan rate 10 mV/s. Insert: Schematic model of Pt_{ML} nanocatalysts.

dx.doi.org/10.1021/jz3016155 | J. Phys. Chem. Lett. 2012, 3, 3480−3485

and (100) planes and have certain surface density of low-coordinated sites. The size, shape, and structure of nanoparticle supports can affect the reactivity, selectivity, and stability of Pt_{ML} in a complex way.[35−38] However, with advanced synthetic nanotechnology methods, designing suitable nanoparticle supports with enhancing properties is quite feasible.

In summary, we described Pt_{ML} catalysts for the electrooxidation of alcohol molecules based on a systematic study involving single-crystal and nanoparticle supports. Oxidation of methanol and ethanol, the reactions of very high importance for electrochemical energy conversion in fuel cells, were taken as examples. Our experimental observations of substrate-induced change in the reactivity of Pt_{ML} fully agree with theoretical predictions. The results demonstrate the potentiality of fine-tuning the catalytic property of Pt_{ML} to fabricate electrocatalysts with enhanced activity and ultralow Pt content. Furthermore, the understanding of this system gained from studies of single-crystal surfaces could be applied successfully to developing nanoparticle catalysts. On the basis of the unique properties of Pt monolayer catalysts, namely, an ultralow Pt content, tunable activity, and selectivity, close to complete Pt utilization, it is likely that this approach will profoundly affect both future research and technologies in electrocatalysis of organic compounds.

■ ASSOCIATED CONTENT

Supporting Information

Materials syntheses, experimental details, Cu UPD, electrochemical measurements, and IR band assignments. This material is available free of charge via the Internet at http://pubs.acs.org.

■ AUTHOR INFORMATION

Corresponding Author

*E-mail: adzic@bnl.gov.

Notes

The authors declare no competing financial interest.

■ ACKNOWLEDGMENTS

This work is supported by U.S. Department of Energy (DOE), Divisions of Chemical and Material Sciences, under the Contract No. DE-AC02-98CH10886. The DFT calculations were carried out using computational resources at the Center for Functional Nanomaterials at Brookhaven National Laboratory.

■ REFERENCES

(1) Lamy, C.; Leger, J.-M.; Srinivasan, S. Direct Methanol Fuel Cells − From a 20th Century Electrochemist'S Dream to a 21st Century Emerging Technology. In *Modern Aspects of Electrochemistry*; Bockris, J.O'M., Eds.; Plenum: New York, 2001; Vol. 3, pp 68−123.

(2) Lamy, C.; Coutanceau, C.; Leger, J.-M. The Direct Ethanol Fuel Cell: a Challenge to Convert Bioethanol Cleanly into Electric Energy. In *Catalysis for Sustainable Energy Production*; Barbaro, P., Bianchini, C., Eds.; WILEY-VCH, Weinheim, Germany, 2009; pp 1−42.

(3) Jusys, Z.; Kaiser, J.; Behm, R. J.; J., R. Methanol Electrooxidation over Pt/C Fuel Cell Catalysts: Dependence of Product Yields on Catalyst Loading. *Langmuir* **2003**, *19*, 6759−6769.

(4) Wang, H.; Jusys, Z.; Behm, R. J. Ethanol Electrooxidation on a Carbon-Supported Pt Catalyst: Reaction Kinetics and Product Yields. *J. Phys. Chem. B* **2004**, *108*, 19413−19424.

(5) Adzic, R. R.; Tripkovic, A. V.; O'Grady, W. E. Structural Effects in Electrocatalysis. *Nature* **1982**, *296*, 137−138.

(6) Xia, X. H.; Iwasita, T.; Ge, F.; Vielstich, W. Structural Effects and Reactivity in Methanol Oxidation on Polycrystalline and Single Crystal Platinum. *Electrochim. Acta* **1996**, *41*, 711−718.

(7) Xia, X. H.; Liess, H.-D.; Iwasita, T. Early Stages in the Oxidation of Ethanol at Low-Index Single Crystal Platinum Electrodes. *J. Electroanal. Chem.* **1997**, *437*, 233−240.

(8) Tripkovic, A. V.; Popovic, K. D. Oxidation of Methanol on Platinum Single Crystal Stepped Electrodes from [100] Zone in Acid Solution. *Electrochim. Acta* **1996**, *41* (15), 2385−2394.

(9) Housmans, T. H. M.; Koper, M. T. M. Methanol Oxidation on Stepped Pt[n(111)×(110)] Electrodes: A Chronoamperometric Study. *J. Phys. Chem. B* **2003**, *107*, 8557−8567.

(10) Lai, S. C. S.; Koper, M. T. M. Electro-Oxidation of Ethanol and Acetaldehyde on Platinum Single-Crystal Electrodes. *Faraday Discuss.* **2008**, *140*, 399−416.

(11) Colmati, F.; Tremiliosi-Filho, G.; Gonzalez, E. R.; Berna, A.; Herrero, E.; Feliu, J. M. The Role of the Steps in the Cleavage of the C−C Bond during Ethanoloxidation on Platinum Electrodes. *Phys. Chem. Chem. Phys.* **2009**, *11*, 9114−9123.

(12) Tian, N.; Zhou, Z.-Y.; Sun, S.-G.; Ding, Y.; Wang, Z. L. Synthesis of Tetrahexahedral Platinum Nanocrystals with High-Index Facets and High Electro-Oxidation Activity. *Science* **2007**, *316*, 732−735.

(13) Chrzanowski, W.; Kim, H.; Wieckowski, A. Enhancement in Methanol Oxidation by Spontaneously Deposited Ruthenium on Low-Index Platinum Electrodes. *Catal. Lett.* **1998**, *50*, 69−75.

(14) Lamy, C.; Rousseau, S.; Belgsir, E. M.; Coutanceau, C.; Leger, J.-M. Recent Progress in the Direct Ethanol Fuel Cell: Development of New Platinum-Tin Electrocatalysts. *Electrochim. Acta* **2004**, *49*, 3901−3908.

(15) Souza-Garcia, J.; Herrero, E.; Feliu, J. M. Breaking the C-C Bond in the Ethanol Oxidation Reaction on Platinum Electrodes: Effect of Steps and Ruthenium Adatoms. *ChemPhysChem* **2010**, *11*, 1391−1394.

(16) Zhang, J.; Vukmirovic, M. B; Xu, Y.; Mavrikakis, M.; Adzic, R. R. Controlling the Catalytic Activity of Platinum-Monolayer Electrocatalysts for Oxygen Reduction with Different Substrates. *Angew. Chem., Int. Ed.* **2005**, *44*, 2132−2135.

(17) Adzic, R. R.; Zhang, J.; Sasaki, K.; Vukmirovic, M. B.; Shao, M.; Wang, J. X.; Nilekar, A. U.; Mavrikakis, M.; Valerio, J. A.; Uribe, F. Platinum Monolayer Fuel Cell Electrocatalysts. *Top. Catal.* **2007**, *46*, 249−162.

(18) Wang, J. X.; Inada, H.; Wu, L.; Zhu, Y.; Choi, Y.-M.; Liu, P.; Zhou, W.-P.; Adzic, R. R. Oxygen Reduction on Well-Defined Core-Shell Nanocatalysts: Particle Size, Facet, and Pt Shell Thickness Effects. *J. Am. Chem. Soc.* **2009**, *131*, 17298−17302.

(19) Kibler, L. A.; El-Aziz, A. M.; Hoyer, R.; Kolb, D. M. Tuning Reaction Rates by Lateral Strain in a Palladium Monolayer. *Angew. Chem., Int. Ed.* **2005**, *44*, 2080−2084.

(20) Kibler, L. A.; El-Aziz, A. M.; Kolb, D. M. Electrochemical Behaviour of Pseudomorphic Overlayers: Pd on Au(111). *J. Mol. Catal. A: Chem.* **2003**, *199*, 57−63.

(21) Hammer, B.; Norskov, J. K. Theoretical Surface Science and Catalysis - Calculations and Concepts. *Adv. Catal.* **2000**, *45*, 71−129.

(22) Greeley, J.; Norskov, J. K.; Mavrikakis, M. Electronic Structure and Catalysis on Metal Surfaces. *Annu. Rev. Phys. Chem.* **2002**, *53*, 319−348.

(23) Markovic, N. M.; Gasteiger, H. A.; Ross, P. N. Copper Electrodeposition on Pt(111) in the Presence of Chloride and (Bi)sulfate: Rotating Ring-Pt(111) Disk Electrode Studies. *Langmuir* **1996**, *11*, 4098−4108.

(24) Brankovic, S. R.; Wang, J. X.; Adzic, R. R. Metal Monolayer Deposition by Replacement of Metal Adlayers on Electrode Surfaces. *Surf. Sci.* **2001**, *474*, L173−L179.

(25) Kim, Y.-G.; Kim, J.-Y.; Vairavapandian, D.; Stickney, J. L. Platinum Nanofilm Formation by EC-ALE via Redox Replacement of UPD Copper: Studies Using *in-Situ* Scanning Tunneling Microscopy. *J. Phys. Chem. B* **2006**, *110*, 17998−18006.

(26) Bae, S.-E.; Gokcen, D.; Liu, P.; Mohammadi, P.; Brankovic, S. R. Size Effects in Monolayer Catalysis—Model Study: Pt Submonolayers on Au(111). *Electrocatalysis* **2012**. DOI: 10.1007/s12678-012-0082-5.
(27) Pedersen, M.Ø.; Helveg, S.; Ruban, A.; Stensgaard, I.; Laegsgaard, E.; Nørskov, J. K.; Besenbacher, F. How a Gold Substrate can Increase the Reactivity of a Pt Overlayer. *Surf. Sci.* **1999**, *426*, 395−409.
(28) Obradovic, M. D.; Tripkovic, A. V.; Gojkovic, S. L. The Origin of High Activity of Pt−Au Surfaces in the Formic Acid Oxidation. *Electrochim. Acta* **2009**, *55*, 204−209.
(29) Iwasita, T. Electrocatalysis of Methanol Oxidation. *Electrochim. Acta* **2002**, *47*, 3663−3674.
(30) Iwasita, T.; Nart, F. C. Identification of Methanol Adsorbates on Platinum − an *in situ* FT-IR Investigation. *J. Electroanal. Chem.* **1991**, *317*, 291−298.
(31) Zhang, J.; Mo, Y.; Vukmirovic, M. B.; Klie, R.; Sasaki, K.; Adzic, R. R. Platinum Monolayer Electrocatalysts for O_2 Reduction: Pt Monolayer on Pd (111) and on Carbon-Supported Pd Nanoparticles. *J. Phys. Chem. B* **2004**, *108*, 10955−10964.
(32) Kowal, A.; Li, M.; Shao, M.; Sasaki, K.; Vukmirovic, M. B.; Zhang, J.; Marinkovic, N. S.; Liu, P.; Frenkel, A. I.; Adzic, R. R. Ternary Pt/Rh/SnO_2 Electrocatalysts for Oxidizing Ethanol to CO_2. *Nat. Mater.* **2009**, *8*, 325−330.
(33) Ferrin, P.; Nilekar, A. U.; Greeley, J.; Mavrikakis, M.; Rossmeisl, J. Reactivity Descriptors for Direct Methanol Fuel Cell Anode Catalysts. *Surf. Sci.* **2008**, *602*, 3424−3431.
(34) Ferrin, P.; Mavrikakis, M. Structure Sensitivity of Methanol Electrooxidation on Transition Metals. *J. Am. Chem. Soc.* **2009**, *131*, 14381−14389.
(35) Arenz, M.; Mayrhofer, K. J. J.; Stamenkovic, V.; Blizanac, B. B.; Tomoyuki, T.; Ross, P. N.; Markovic, N. M. The Effect of the Particle Size on the Kinetics of CO Electrooxidation on High Surface Area Pt Catalysts. *J. Am. Chem. Soc.* **2005**, *127*, 6819−5829.
(36) Lee, S. W.; Chen, S.; Suntivich, J.; Sasaki, K.; Adzic, R. R.; Yang, S.-H. Role of Surface Steps of Pt Nanoparticles on the Electrochemical Activity for Oxygen Reduction. *J. Phys. Chem. Lett.* **2010**, *1*, 1316−1320.
(37) Tarnowski, D. J.; Korzeniewski, C. Effects of Surface Step Density on the Electrochemical Oxidation of Ethanol to Acetic Acid. *J. Phys. Chem. B* **1997**, *101*, 253−258.
(38) Cai, Y.; Ma, C.; Zhu, Y.; Wang, J. X.; Adzic, R. R. Low-Coordination Sites in Oxygen-Reduction Electrocatalysis: Their Roles and Methods for Removal. *Langmuir* **2011**, *27*, 8540−8547.

Supplementary Information for

Platinum Monolayer Electrocatalysts for Anodic Oxidation of Alcohols

M. Li, P. Liu, R. R. Adzic*

Department of Chemistry, Brookhaven National Laboratory, Upton, NY 11973

*To whom correspondence should be addressed. E-mail: adzic@bnl.gov

This file includes:

Methods

Figs. S1 to S3

Table S1

References

Methods

Catalysts Syntheses.

Six single crystals Au(111), Pd(111), Rh(111), Ru(0001), Ir(111), and Pt(111) of 8mm in diameter were obtained from Metal Crystals and Oxides, and the single crystals surfaces were oriented to better than 0.2°. The surfaces were prepared following standard procedures,[1] and then they were mounted in a holder for work in a ‘‘hanging meniscus’’ configuration or into the FTIR cell. Quality of single crystal surfaces were examined by cyclic voltammogram and a Pt monolayer was deposited by displacing an underpotentially deposited Cu monolayer layer on single crystal surfaces (further details in Fig. S1).

Commercial carbon-supported nanoparticle catalysts Pt/C, Au/C and Pd/C were obtained from ETEK. Pd_9Au_1 alloy nanoparticles was synthesized using wet impregnation of XC-72 carbon by Pd and Au chlorides, dried, and reduced using $NaBH_4$ solution. Pt_{ML} was deposited on Au/C, Pd/C and Pd_9Au_1/C by galvanic displacement of a Cu UPD layer.

Electrochemical Measurements.

All electrochemical measurements were carried out under room temperature. Current density data were reported with surface area normalized in terms of the electrochemical active surface area (ECSA) that was determined by the charge of stripping one Cu UPD monolayer on Pt(111) or Pt_{ML} (assuming 480 $\mu C/cm^2_{Pt}$). The potentials given in this paper were referenced to that of the Ag/AgCl electrode.

IRRAS.

In situ IRRAS studies were carried out with a Nicolet Nexus 670 Fourier-transform infrared (FTIR) spectrometer equipped with a mercury cadmium telluride (MCT) detector cooled with liquid nitrogen. An unpolarized light beam was used. The spectral resolution was set to 8 cm^{-1} and 128 interferograms were together added to each spectrum. Spectra are given in absorbance units defined as $A = -\log(R/R_0)$, where R and R_0 represent the reflected infrared intensities corresponding to the sample and reference single-beam spectrum, respectively. The reference spectrum was collected at 0.1 V in the same solution (0.5M methanol or ethanol in 0.1M $HClO_4$). Pt_{ML}/Au(111) electrode was employed in IRRAS study. A ZnSe hemisphere was used as the infrared window.

DFT calculation.

DFT calculations were conducted using DMol3,[2,3] which utilized the effective core potentials, double-numerical basis set with polarization functions and GGA-PW91 for the exchange and correlation functional.[4] A global orbital cutoff of 5.5 Å was used. Brillouin-zone integrations were performed on a grid of 4×4×1 Monkhorst-Pack special k-points. The metal surface was modeled by a four-layer slab with a (2×2) unit cell respectively, which was separated by enough vacuum space. The bottom two layers of atoms were fixed in their optimized bulk positions while the other layers were allowed to relax with the adsorbates.

Fig. S1. Preparation of Pt monolayer catalysts: voltammetry curves for the underpotential deposition of Cu on single crystal surfaces in 0.05 M H_2SO_4 with 0.05M $CuSO_4$, and for the respective single crystal surface in 0.1M $HClO_4$; sweep rate 10 mV/s. (a) Au(111); (b) Pd(111); (c) Ir(111); (d) Rh(111); (e) Ru(0001).

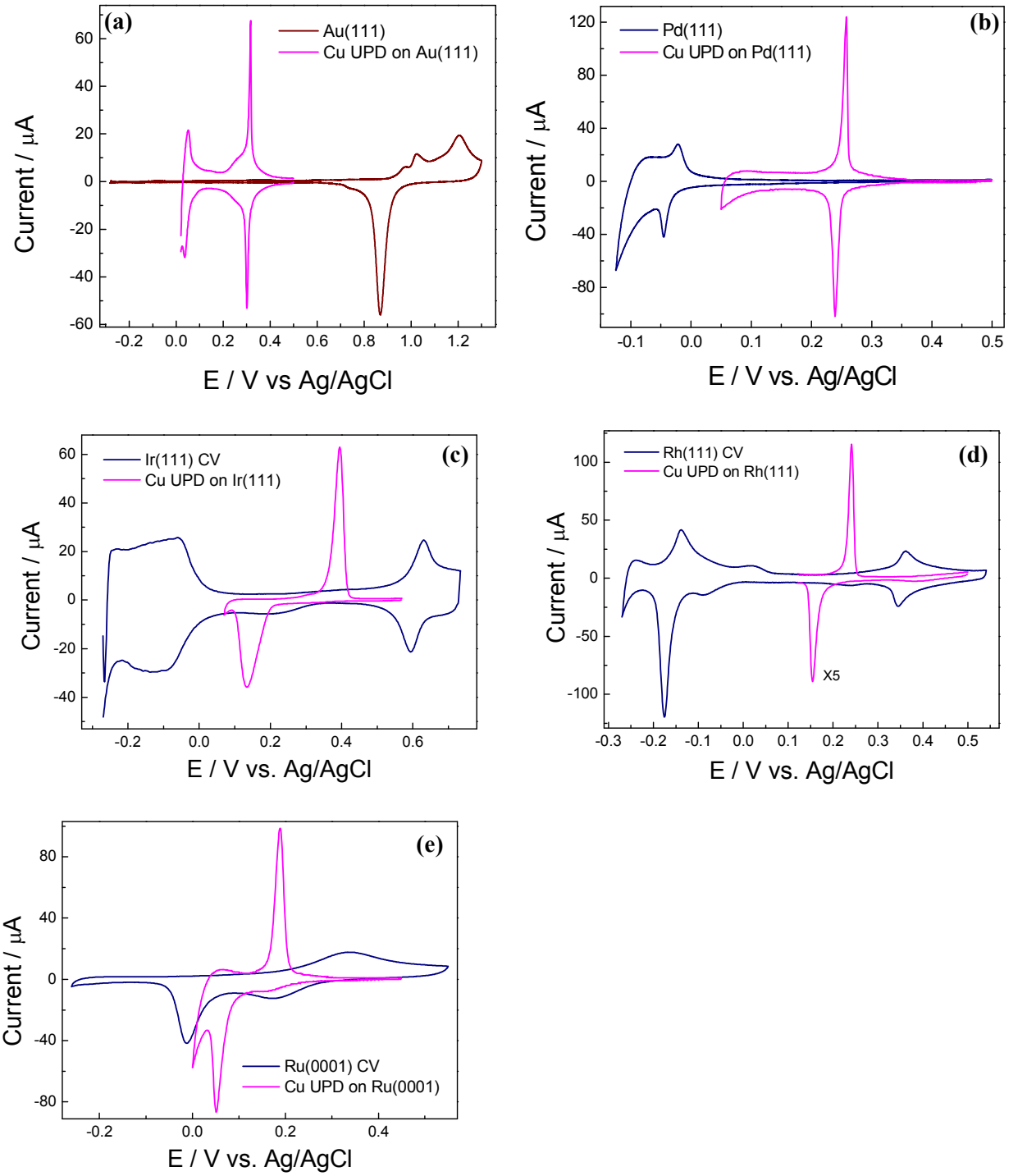

Fig. S2. Cyclic voltammogram of all catalytic surfaces (viz. Pt(111), Pt_{ML}/Au(111), Pt_{ML}/Pd(111), Pt_{ML}/Ir(111), Pt_{ML}/Rh(111), and Pt_{ML}/Ru(0001)) during MOR (a) and EOR (b) in 0.1M $HClO_4$ containing 0.5M methanol or 0.5M ethanol with a sweep rate of 10mV/s.

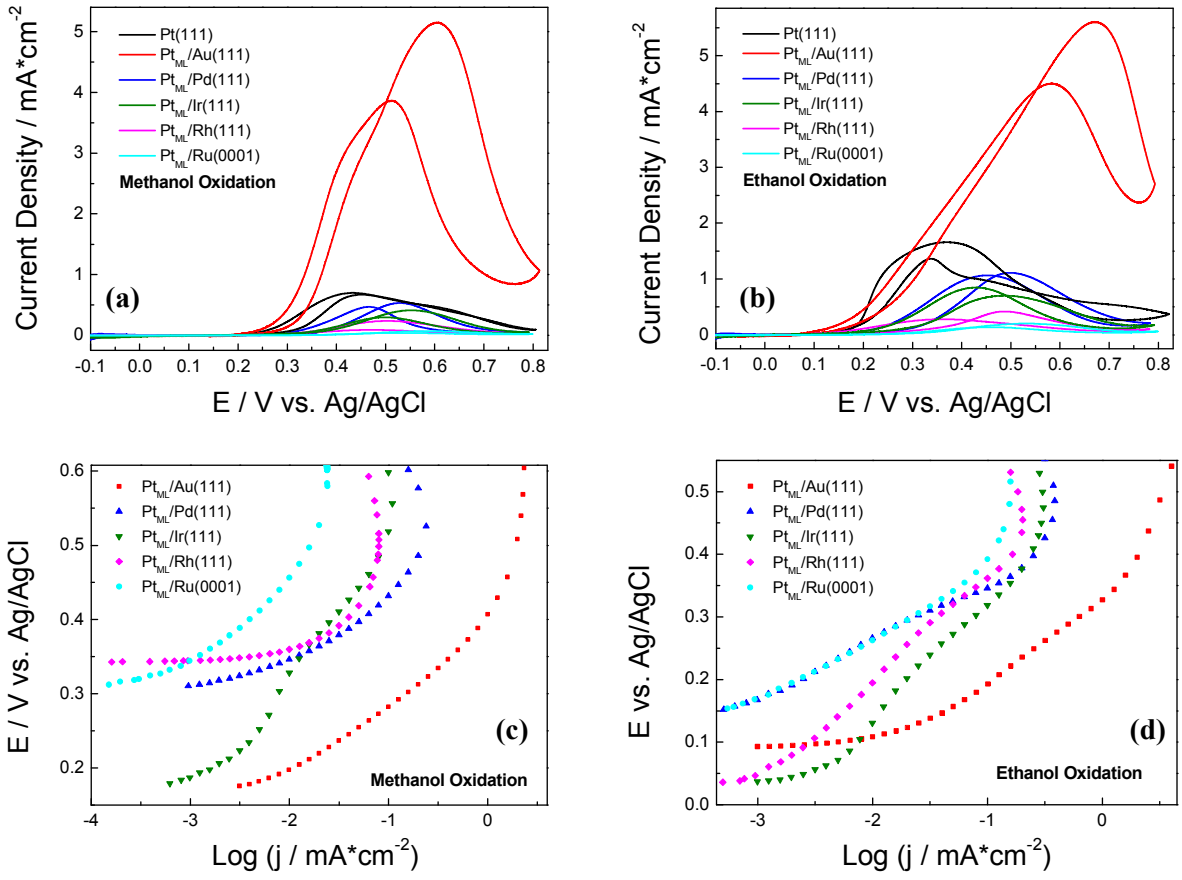

Fig. S3. Cyclic voltammetry curves of a Pt monolayer on a Au(111) surface (Pt_{ML}/Au(111)) obtained by galvanic displacement of the Cu monolayer, a Pt monolayer on a Pd(111) surface (Pt_{ML}/Pd(111)) and a Pt(111) surface. The electrolyte solution is 0.1 M $HClO_4$ and the sweep rate is 10mV/s.

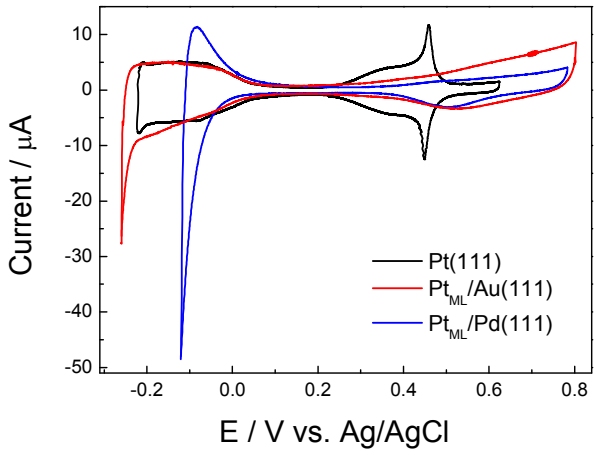

Table S1. *In Situ* IRRAs spectra band assignments[5,6]

Wavenumber/cm^{-1}	Assignment
2343	CO_2 asymmetric stretching
2090	CO linear bonding
1705	C=O stretching of CH_3CHO and CH_3COOH in solution
1620-1635	C=O stretching of adsorbed acetaldehyde and acetyl
~1598	H-O-H deformation of adsorbed water
1396-1410	O-C-O stretching of adsorbed acetate
~1350	CH plane bending of adsorbed acetate
1280	C-O stretching of CH_3COOH in solution
1368	CH_3 symmetric deformation and C-H wagging in CH_3CHO

References

[1] Zhang, J., Mo, Y., Vukmirovic, M. B., Klie, R., Sasaki, K., Adzic, R. R. Platinum monolayer electrocatalysts for O_2 reduction: Pt monolayer on Pd(111) and on carbon-supported Pd nanoparticles. *J. Phys. Chem. B* **2004**, *108*, 10955-10964.

[2] Delley, B. An all-electron numerical-method for solving the local density functional for polyatomic-molecules. *J. Chem. Phys.* **1990**, *92*, 508-517.

[3] Delley, B. From molecules to solids with the DMol(3) approach. J. Chem. Phys. 113, 7756-7764 (2000).

[4] Perdew, J. P., Wang, Y. Accurate and simple analytic representation of the electron-gas correlation-energy. Phys. Rev. B 45, 13244-13249 (1992).

[5] Li, M., Kowal, A., Sasaki, K., Marinkovic, N. S., Su, D., Korach, E., Liu, P., Adzic, R. R. Ethanol oxidation on the ternary Pt–Rh–SnO2/C electrocatalysts with varied Pt:Rh:Sn ratios. *Electrochimica Acta* **55**, 4331–4338 (2010).

[6] Shao, M., Adzic, R. R. Electrooxidation of ethanol on a Pt electrode in acid solutions: *in situ* ATR-SEIRAS study. *Electrochimica Acta* **50**, 2415–2422 (2005).